CHAPTER EIGHT

Applications of Electrochemical Machining

The main attractions of ECM that were outlined in Chapter 1 are its ability to machine very hard metals without causing tool wear and structural damage to the workpiece, and to form complex shapes which are difficult to produce by conventional methods. Its main drawbacks are the high capital cost of the equipment, the cost of tooling, and corrosion problems, which shorten the working life of the equipment. Because of these features, ECM has been used most successfully in aerospace applications where the advantages of using the process, often for a large number of components, outweigh its disadvantages.

Nonetheless, the benefits of ECM are now becoming recognised in other industries, and the process is being used in an increasing number of ways. In some of these applications, the main characteristics of the process are the attraction. In others, ECM has replaced established machining methods because it has been found to give superior results, or to be more economic. Several examples, drawn mainly from these industries, are now discussed which illustrate many of the features of the process studied in the preceding chapters.

8.1 Electrochemical shaping

The application, shown in Fig. 8.1, illustrates the basic principles of ECM, described in Chapter 1. A brass, and occasionally, copper tungsten cathode tool has been used to machine a solid block of stainless steel to the shape required for a knitting machine cam. An applied voltage of 15 to 20 V was applied between the two electrodes,

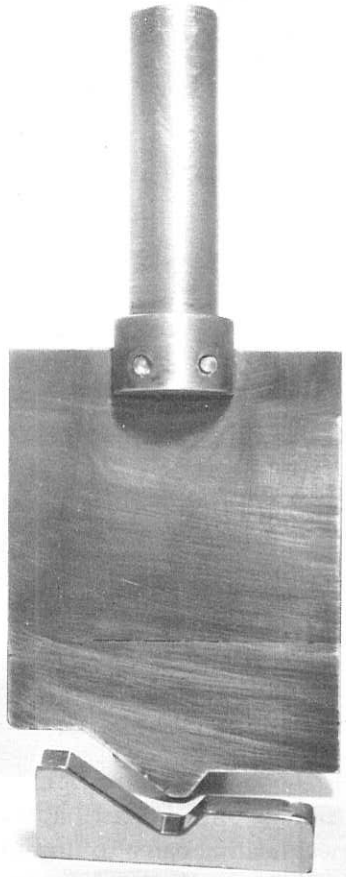

Fig. 8.1 Electrochemical shaping of stainless steel knitting machine cam (By permission of Healy of Leicester Ltd.)

and the cathode feed-rate was 0·03 mm/s. Under equilibrium machining conditions, the current and current density were 26 A and roughly 78 A/cm^2 respectively, the gap width being 0·25 mm. For these values of the process variables, the shape could be formed on the anode in 270 s.

A requirement of this operation was close tolerance of the machined component – to within 0·1 mm. To achieve this accuracy, a 30% (w/w) $NaNO_3$ electrolyte was chosen. This electrolyte provides good dimensional control without involving the greater hazards met with $NaClO_3$ solution, even though the latter electro-

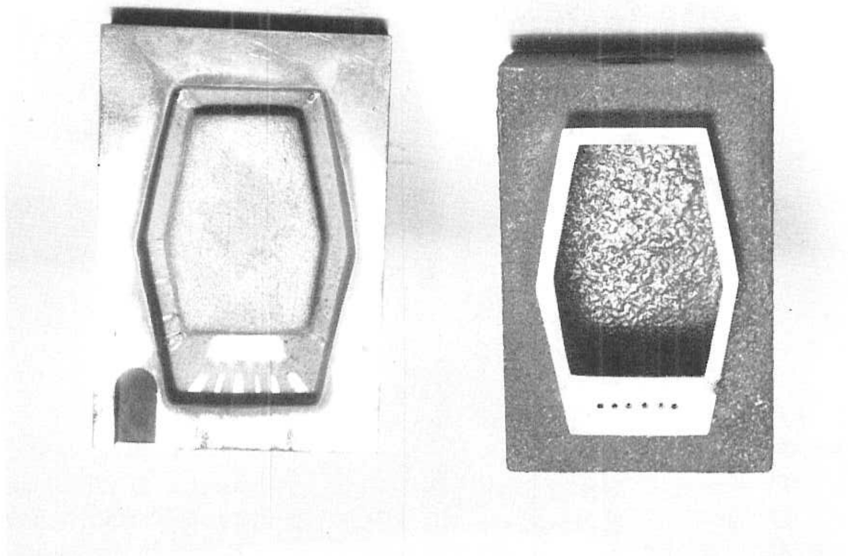

Fig. 8.2 Cathode tool (right) used for electrochemical cavity-sinking preparation of die steel master for rubber moulds; polished streaks on work-piece (left) caused by flow separation (By permission of Healy of Leicester Ltd.)

lyte offers better dimensional control (see Chapter 4). Since hydrogen gas and electrical heating can also upset the accuracy of machining, as discussed in Chapter 5, the electrolyte was maintained at a high inlet temperature of 45°C, and pumped across the breadth (12 mm) of the specimen, the inlet pressure being 1·66 MN/m^2 and the flow-rate (0·76 to 1·14) x 10^{-3} m^3/s.

8.2 Electrolyte flow separation

In the first example, the care taken to ensure a suitable flow path for the electrolyte was pointed out. Good flow conditions are not always readily available in practice, and Fig. 8.2 illustrates a case where poor conditions have led to flow separation and to the termination of machining.

The cathode shape on the right was to be used for a cavity sinking operation at 0·01 mm/s and 15 V to produce the anode shape

on the left. The die steel workpiece so formed was then to be used as a master for the manufacture of rubber moulds.

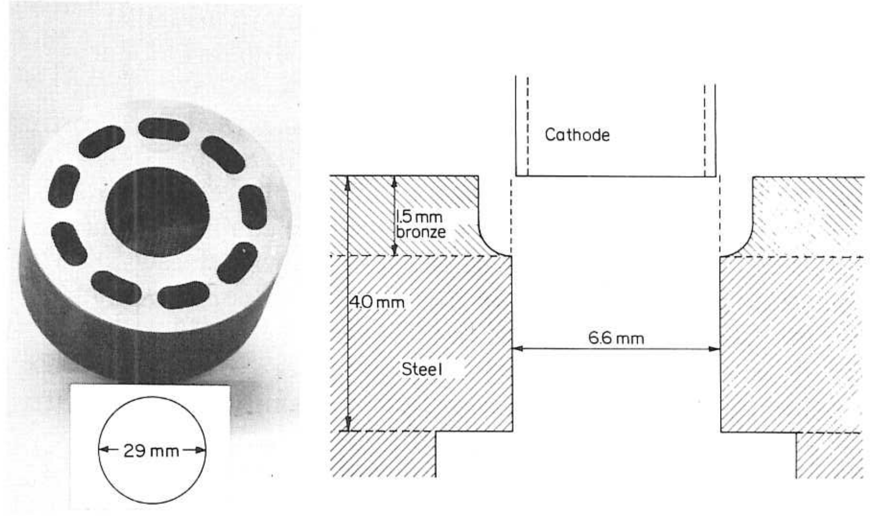

(a) (b)

Fig. 8.3(a) Anode workpiece of bronze and steel, used in electrochemical drilling of kidney-shaped slots in pump body (By permission of Lucas Aerospace Co. Ltd., Netherton). (b) Increased overcut through bronze due to difference in machining characteristics of bronze and steel

A 20% (w/w) NaCl solution was introduced through the entry port (top right) at a pressure of 1·38 MN/m^2 and a flow-rate of (0·76 to 1·14) x 10^{-3} m^3/s. The aim was to use the cavity in the cathode as a pressurised chamber for the electrolyte solution during ECM, the outlet for the electrolyte flow being the six holes shown at the foot of the cathode. This configuration, however, led to an uneven flow distribution which caused the polished streaks on the surface of the anode workpiece. Since the current was high – about 700 A – the gap width must have been small, and the irregularities jutting out into the machining gap also caused sparking between the electrodes. The influence of hydrodynamic phenomena (Chapter 2) on surface finish has been described in Chapter 4, and the limitations which they impose on the rate of machining have been discussed in Chapter 5.

8.3 Contrasting metal removal rates

In Chapters 1 and 4, the different rates of machining achieved with different metals were studied in detail. A practical example of the difficulties encountered in machining through two dissimilar materials has occurred in the electrochemical drilling of kidney-shaped slots in a bronze–steel pump body. (Fig. 8.3(a)). In this operation, the head of the cathode tool first met the bronze part of the workpiece, which was 1·5 mm deep (Fig. 8.3(b)). Below the bronze, the tool next encountered steel. The change in material being machined was observed as an increase in equilibrium current. The difference in the machining rates of the two metals was also apparent from the change in overcut, which was considerably less for the steel part of the workpiece. This effect is noticeable in Fig. 8.3(b) as the step at the junction of the bronze and steel.

This example also usefully demonstrates some other aspects of ECM described in Chapters 4, 5 and 7. First, an electrolyte was chosen which gave good dimensional control. The electrolyte was maintained at a constant temperature and pumped at an established flow-rate and pressure in a 'reversed-flow' direction: that is, first down the outer, insulated wall of the cathode, then across the machining face and up through the slot in the tool. This technique diminishes considerably the unwanted effects of hydrogen gas and electrical heating (Chapter 5) by reducing the extent of the flow path over which they can have any influence.

8.4 Mechanical properties of electrochemically machined parts

A benefit of ECM which was explored in Chapters 1 and 4 was that the process does not affect the mechanical properties of machined metals, and moreover, that removal of metal leaves the material in a natural, undistorted state.

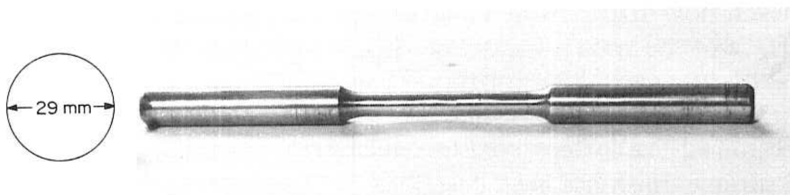

Fig. 8.4 Steel tensile test specimen prepared by electrochemical turning (By permission of Healy of Leicester Ltd.)

This feature has been utilised in the preparation of tensile test specimens for metallurgical work (Fig. 8.4). Here the necked section of the specimen was produced by an electrochemical turning operation in which the steel anode workpiece was rotated on its long axis whilst a cathode tool was moved along it at a rate of 0·006 mm/s. The front gap between the two electrodes was about 0·25 mm, the applied voltage, current, and average current density being 15 V, 100 A, and 78 A/cm^2 respectively. The inlet temperature of the 20% (w/w) NaCl electrolyte was maintained at 35°C, the inlet pressure and flow-rate being 0·69 MN/m^2 and (0·76 to 1·14) x 10^{-3} m^3/s respectively.

8.5 Electrochemical smoothing of irregularities

An increasingly popular application of ECM is anodic smoothing, the main features of which were discussed in Chapter 6. An advantage of this technique in practice is that often no cathode tool movement is needed. Figure 8.5(a) illustrates an example in which surface irregularities had to be removed from the external spline of a shift hub sleeve. Figure 8.5(b) is a schematic diagram of the shape of the stationary cathode tool and configuration of electrodes used for the electrochemical removal of each irregularity whose height was 0·25 mm. The initial gap width between the two electrodes was 0·5 mm. The applied potential difference was 12 V, and with a current of 250 A, about 0·08 mm of metal from the irregularity could be removed in 3 s.

A 30% (w/w) $NaNO_3$ electrolyte at 30°C was used in this work because its good dimensional control restricted ECM mainly to the region of the surface irregularity. The pressure at inlet required for this operation was only about 202 kN/m^2, the flow-rate being about 0·76 x 10^{-3} m^3/s. To minimise the unwanted effects of gas and heating, the electrolyte was caused to flow across the short face of the anode. Figure 8.5(c) shows the configuration of cathode electrodes used for the simultaneous dissolution of all such irregularities on the workpiece. Figure 8.5(d) illustrates the location of both the anode and cathode fixtures.

8.6 Cathode design

Figure 8.6 shows a titanium alloy blade whose complex shape has been produced by ECM. A current of 5000 A (current density

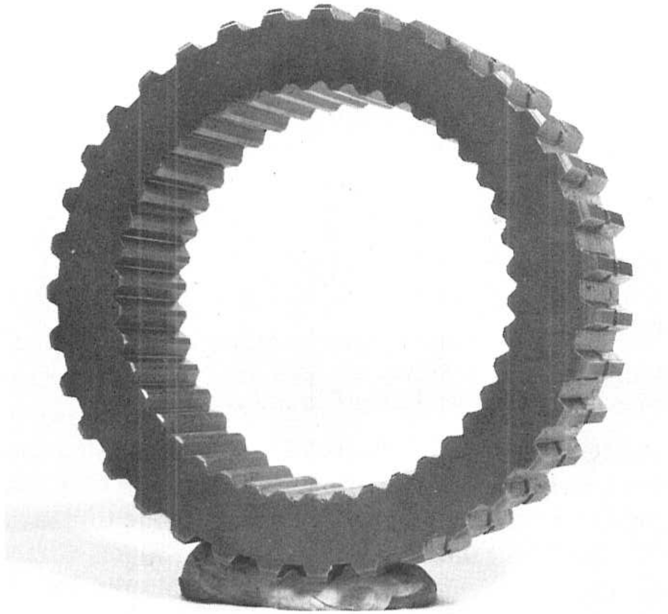

(a)

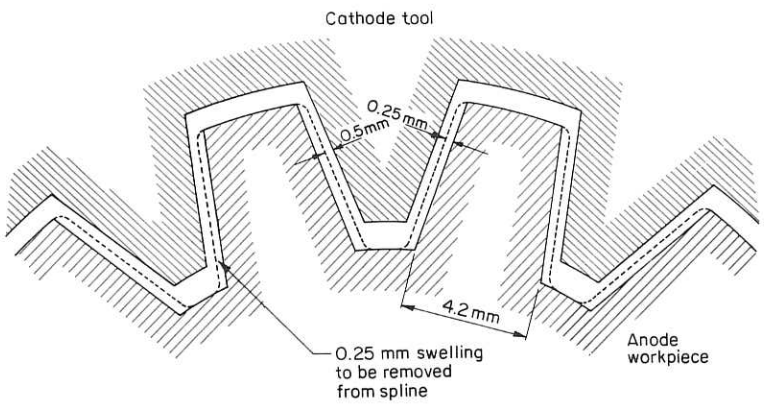

(b)

Fig. 8.5(a) Surface irregularities on external spline of case hardened steel shift hub sleeve (By permission of Turner Manufacturing Co. Ltd., Wolverhampton). (b) Configuration of cathode tool and external spline carrying surface irregularity

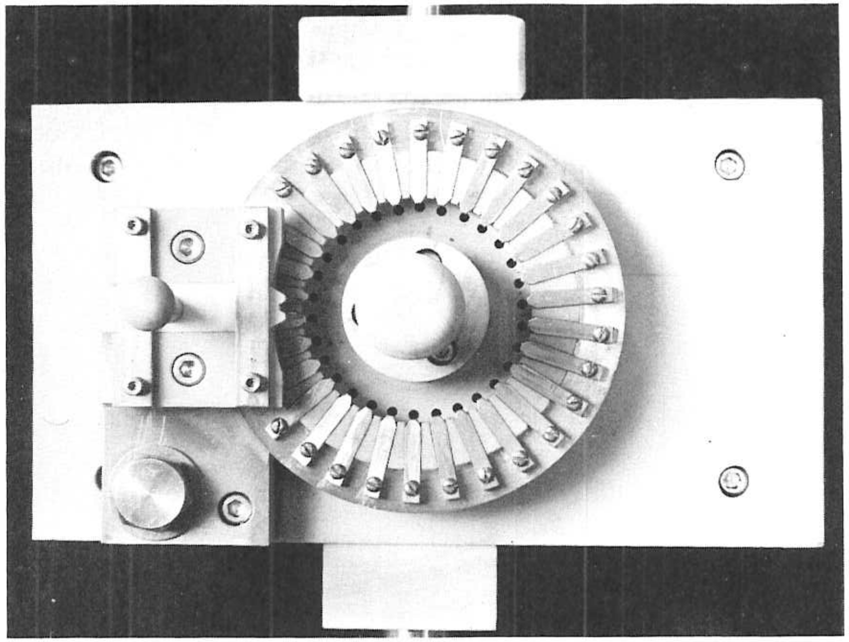

(c)

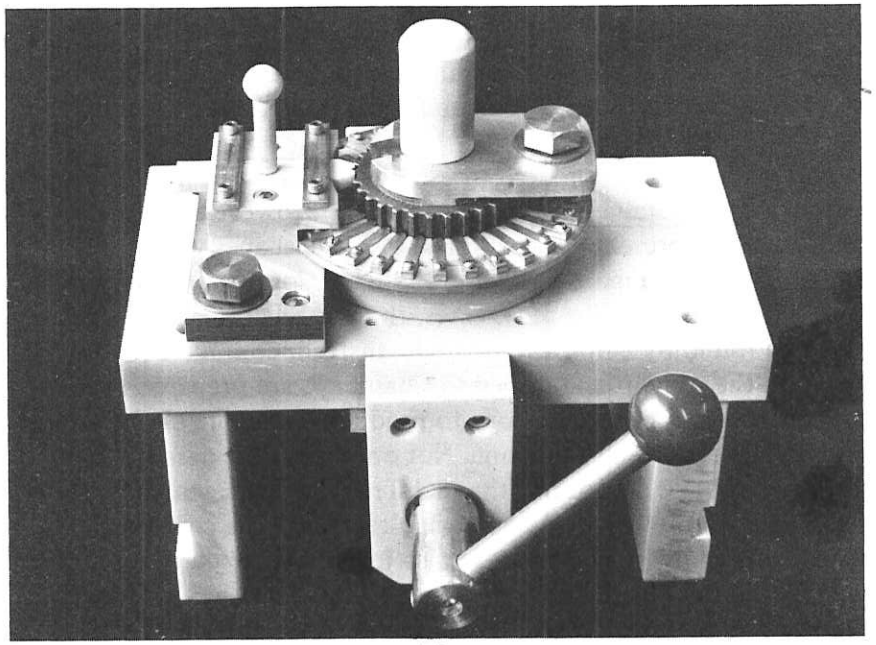

(d)

Fig. 8.5(c) Multiple cathode tool system for electrochemical dissolution of workpiece irregularities (By permission of Turner Manufacturing Co. Ltd., Wolverhampton). (d) Configuration of multiple cathode tools and anode workpiece for electrochemical removal of surface irregularities (By permission of Turner Manufacturing Co. Ltd., Wolverhampton)

186 A/cm^2) at 10 V was used to machine this tough metal. The cathode feed-rate was 0·05 mm/s and the depth of metal machined was 6·35 mm; the equilibrium (end) gap width was 0·15 mm. Good dimensional control was maintained during machining by use of a

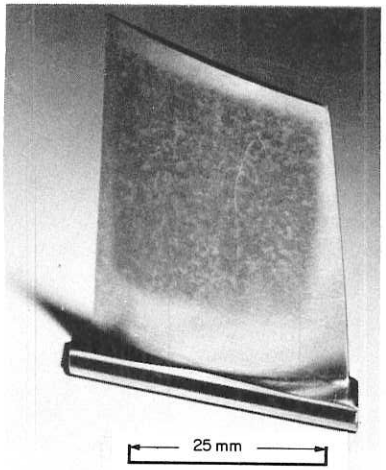

Fig. 8.6 Titanium alloy blade (By permission of Herbert Machine Tools Ltd., Lutterworth)

30% (w/w) $NaNO_3$ electrolyte, the temperature of which at inlet was 40°C. The pressures at inlet and outlet were, respectively, 1·4 MN/m^2 and 340 kN/m^2.

The shape of the cathode tool used to perform this machining operation was obtained by empirical means. However, this anode workpiece is representative of a class of blade shapes which are often much larger, more complex, and have closely defined contours in three dimensions. For these cases, the cathode tool shape cannot easily be found by empirical methods. Instead, computer programs, based on the principles outlined in Chapter 7, are prepared to predict the cathode tool form necessary to produce the anode blade shape. The problem is not a simple one. Not only must the data needed for the program take account of the metal removal rate, which is dependent on the usual process variables and on the choice of a suitable electrolyte, but it should also include some correction for the taper in the machining gap caused by hydrogen gas and electrical heating (Chapter 5). These effects have so far only been predicted for comparatively simple electrode shapes. Much remains to be done to extend these studies to the other electrode configurations encountered in practice.

Bibliography

Wilson, J. F., *Practice and Theory of Electrochemical Machining*, Wiley-Interscience, New York (1971).

Appendix 1 Constituents (percentages) and dimensions of principal metals discussed in Chapter 4

Metal	Al	Be	Bi	Cd	C	Co	Cr	Cu	Fe	Mg	Mo	Mn	Nb	Ni	P	S	Si	Sn	Ti	U	W	Zn	Other information: Ref. no., shape of specimen face. (C circular, R rectangular, S square, T tubular), dimensions (mm)
Nickel					0·15 max.			0·25 max.	0·4 max.	0·2 max.		0·35 max.		bal.		0·01 max.	0·15 max.						2, C, 33 dia.
Copper			0·05					99								0·05							2, C, 33 dia.
Copper								⩾99·9															3, S, 3 x 3
Nimonic 75					0·1		19·5	0·5	5·0			1·0		72·5			1·0		0·4				2, C, 33 dia.
Monel					0·3			31·7	2·5			2		63			0·5						3, C, 33 dia.
Nimonic 80	constituents not given																						6, R, 50 x 12·5
Mild steel	Type 1020 (U.S.)								100 (assumed)														7, T, 15·9 mm^2 area
Nickel–chromium	alloy type 56 NiCr MoV7 (Ger)																						8
Mild steel	constituents not given								100 (assumed)														11, C, 20 mm^2 area
Carbon steel					0·06				bal.			0·38					0·01						16, C, 13 dia, (polarisation work)
					0·25				bal.														
					0·34				bal.			0·76					0·30						
					0·52				bal.			0·81					0·26						16, S, 25 x 25 (ECM work)
					0·78				bal.			0·63					0·18						
					0·99				bal.			0·23					0·64						
					1·26				bal.			0·22					0·23						
Cast iron					3·03				bal.			0·53		0·1		0·1	2·22						18, C, 33 dia.
Ni–Cr Steel	Type Carpenter R.D.S. (U.S.)																						19, T, 7·2 (ins. dia.) (cathode) 19, C, 6·35 dia. (anode)
Iron				0·03					bal.			0·36		0·02	0·016		trace	0·007					20, R, 5 x 20
Copper								99·99															21, S, 3 x 3
Copper								99·99															21, C, 10^3 mm^2 area
Nickel						1·3								bal.									5, C, 19·1 dia.
Stainless steel					0·08		17·81					0·88		8·78	0·03	0·17	0·58		0·46				23, R, 12·5 x 50
Soft iron	Constituents not given																						27, C, 1·3 dia.
Steel	Type 1020 (U.S.)								100 (assumed)														29, as Ref. 19
Nickel																							32, R, 12·5 x 22·9
Nickel														99·5									33, as Ref. 19
Mild steel	Type 1020 (U.S.)																						33, as Ref. 19
Nickel			0·004		0·06	0·23		0·01	0·06	0·08		0·23		bal.		0·003	0·04						34, C, 6·3 dia.
Nimonic 80A	1					2	68		5			1		bal.			1		2				34, C, 6·3 dia.